Laser Spectroscopy on Bunched Radioactive Ion Beams

Jon Billowes

University of Manchester

THE UNIVERSITY of MANCHESTER

Balkan School on Nuclear Physics, Bodrum 2004

Lecture notes available at: www.man.ac.uk/dalton/files

Lecture 1.

1.1 Nuclear moments

1.2 Hyperfine interaction in free atoms

1.3 Lasers and laser spectroscopy

1.4 Collinear-beams laser spectroscopy

Lecture 2.

2.1 Ion beam cooling and bunching

2.2 Experiments with bunched beams

2.3 Laser ionization techniques

1.1 Nuclear Moments

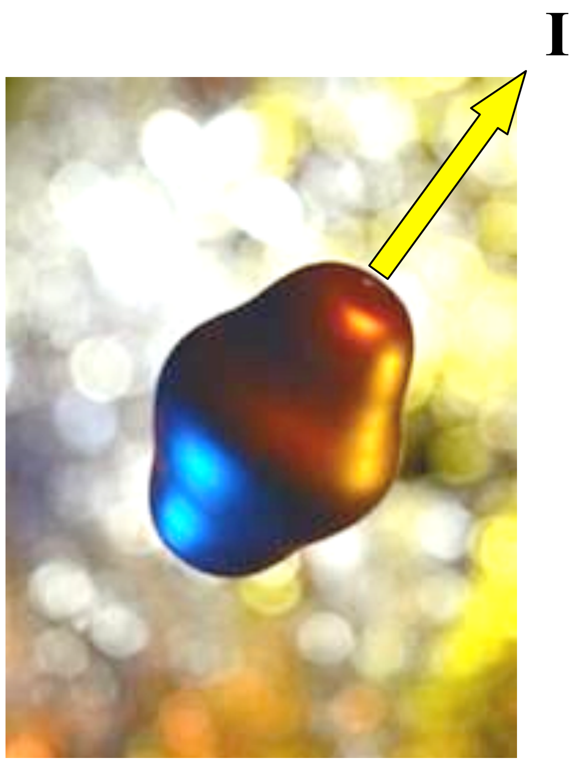

Laser spectroscopy on atomic transitions can measure the following properties of nuclear states (if they live longer than a few milliseconds):

Nuclear Charge – elements have characteristic spectral lines

$$Q = Ze = \int_0^\infty \rho_n(\mathbf{r})\,\mathrm{d}\tau$$

Nuclear Size – or, to be more precise, the mean square nuclear charge radius

$$\langle r^2 \rangle = \frac{1}{Ze}\int_0^\infty \rho_n(\mathbf{r}) r^2 \mathrm{d}\tau$$

Nuclear Shape – the quadrupole moment

$$eQ = \int_0^\infty \rho_n(\mathbf{r})(3z^2 - r^2)\,\mathrm{d}\tau = \int_0^\infty 2\rho_n(\mathbf{r})\, r^2\, P_2(\cos\theta)\,\mathrm{d}\tau$$

Nuclear Spin

$$\mathbf{I} = \sum_{\mathbf{i}} (\mathbf{l_i} + \mathbf{s_i})$$

Nuclear magnetic moment

$$\hat{\mu}_I = \sum_i (g_l^i \mathbf{l_i} + g_s^i \mathbf{s_i}) = g\mathbf{I}\mu_N$$

The magnetic (dipole) moment μ

$$\hat{\mu}_I = \sum_i (g_l^i \mathbf{l_i} + g_s^i \mathbf{s_i})$$

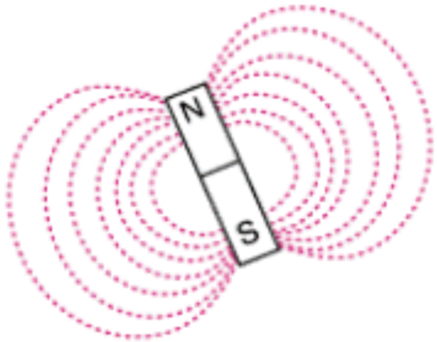

Contributions from orbiting charge and intrinsic spin

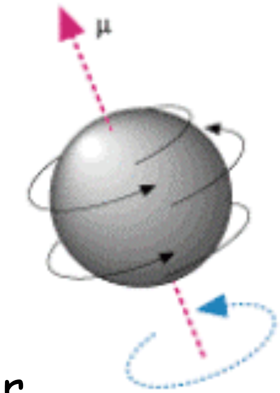

Protons:	g_l = +1	g_s = +5.587
Neutrons:	g_l = 0	g_s = -3.826

The magnetic dipole moment of a state of spin I
= expectation value of the z-component of the dipole operator

$$\mu =< I, m = I|\hat{\mu}_z|I, m = I >$$

The magnetic moment (or g-factor) therefore tells us about the valence nucleon orbits and couplings (filled shells couple to spin=0 and do not contribute).

Spectroscopic Quadrupole Moment

Experiments measure the maximum "projection" of the intrinsic electric quadrupole moment along the quantization axis

$$Q_s = Q_0 \, P_2(\cos\,\theta)_{m=I}$$

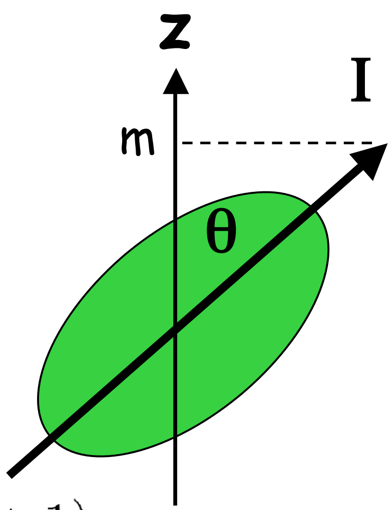

Using angular momentum algebra, we get $Q_s = Q_0 \frac{3K^2 - I(I+1)}{(I+1)(2I+3)}$

K is the projection of the spin I along the symmetry axis. Note for nuclear spin I=0 and I=1/2 the spectroscopic quadrupole moment vanishes even if the intrinsic shape is deformed.

The intrinsic moment can be related to the quadrupole deformation parameter:

$$Q_0 \approx \frac{3Zr_0^2}{\sqrt{5\pi}} \langle\beta_2\rangle (1 + 0.36\langle\beta_2\rangle)$$

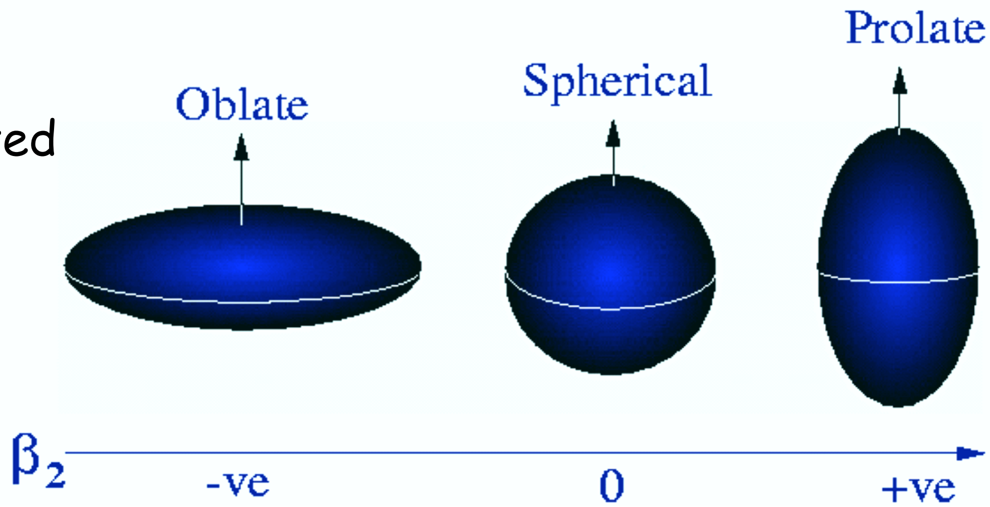

1.2 Hyperfine Interactions in free atoms

Hyperfine interaction = the interaction of nuclear magnetic and electric moments with electromagnetic fields.

We will consider the effect on an atomic orbit of spin J

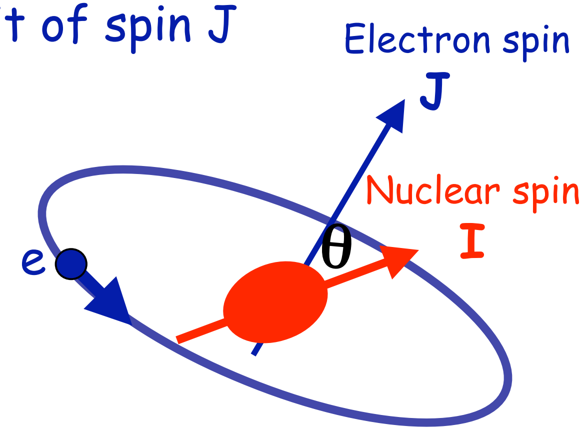

The atomic and nuclear spins couple to form the total angular momentum

F = **I** + **J**

Each state J has several F-states:

$$|I-J| \leq F \leq I+J$$

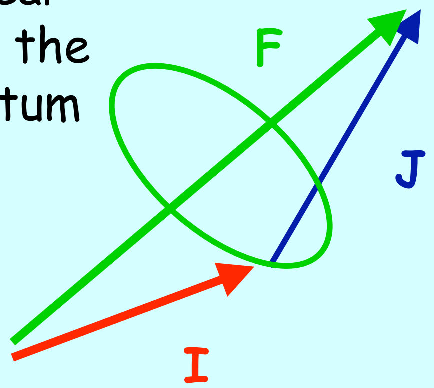

The interaction energy depends on the angle θ thus for the same **I** and **J**, the different F-states are at slightly different energies:

Magnetic dipole interaction

$$E = -\boldsymbol{\mu} \cdot \mathbf{B}_e = -\mu B_e \cos\theta$$

Electric quadrupole interaction

$$E = \tfrac{1}{4} e Q_0 V_{JJ} P_2(\cos\theta)$$

Magnetic dipole interaction

$$E = -\boldsymbol{\mu} \cdot \mathbf{B_e} = -\mu B_e \cos\theta$$

Since $\boldsymbol{\mu} = g\mathbf{I}\mu_N$ and $\mathbf{B}_e = -(\frac{B_e}{J})\mathbf{J}$

then interaction Hamiltonian can be expressed as $H_m = (\frac{gB_e\mu_N}{J})\mathbf{I.J} = A\mathbf{I.J}$

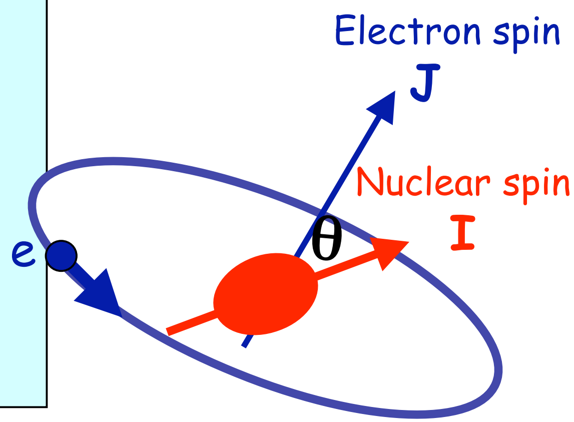

The different energy shifts of the different F-states are then $\Delta E = \langle IJF \mid H_m \mid IJF \rangle = A\langle \mathbf{I.J} \rangle$

where $\langle \mathbf{I.J} \rangle = \frac{1}{2}\langle F^2 - I^2 - J^2 \rangle = \frac{1}{2}[F(F+1) - I(I+1) - J(J+1)]$

B_e, the magnetic field at the nucleus produced by the atomic electrons can be calibrated by measuring the energy shifts for a isotope of known magnetic moment.

Electric quadrupole interaction

In a uniform electric field the energy of an electric quadrupole moment is independent of angle and therefore there is no quadrupole interaction

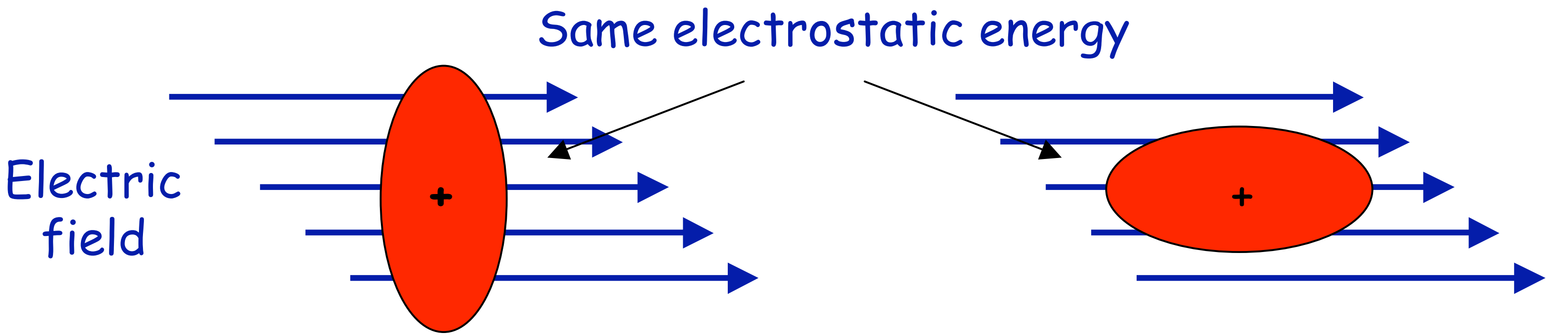

There is an angle-dependence in an electric field gradient

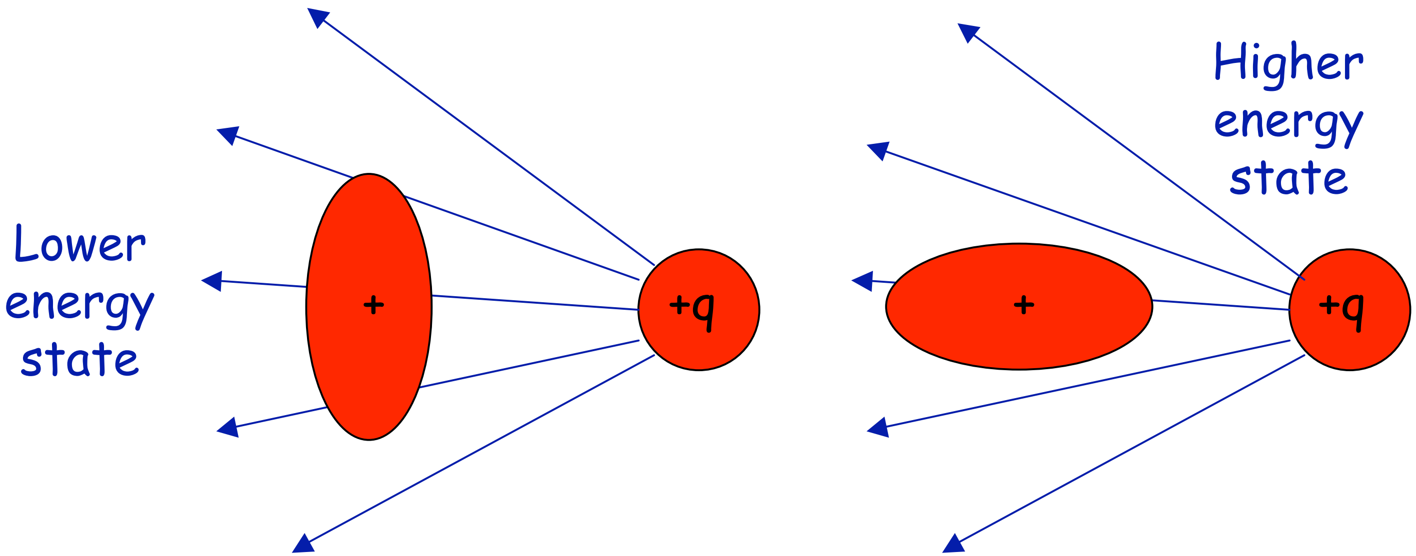

Electric quadrupole interaction

$$E = \tfrac{1}{4}\, e\, Q_0\, V_{JJ}\, P_2(\cos\theta)$$

Electric field gradient along J-direction due to atomic electrons.

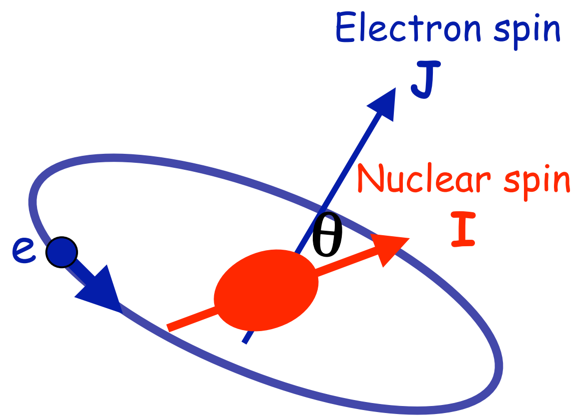

Energy shifts of the F-states are then

$$\Delta E_Q = \frac{B}{4} \frac{\frac{3}{2}C(C+1) - 2I(I+1)J(J+1)}{I(2I-1)J(2J-1)}$$

where $C = [F(F+1) - I(I+1) - J(J+1)]$

$$B = eQ_s \langle \frac{\partial^2 V}{\partial Z^2} \rangle = eQ_s V_{JJ}$$ is the hyperfine factor measured by experiment.

The electric field gradient V_{JJ} may be calibrated with an isotope with know Q_s

Isotope Shift and Hyperfine Structure (example: J=1, I=3/2)

Point nucleus + Finite size of nucleus + Magnetic dipole + Electric quadrupole + higher multipoles (too small to consider in laser measurements)

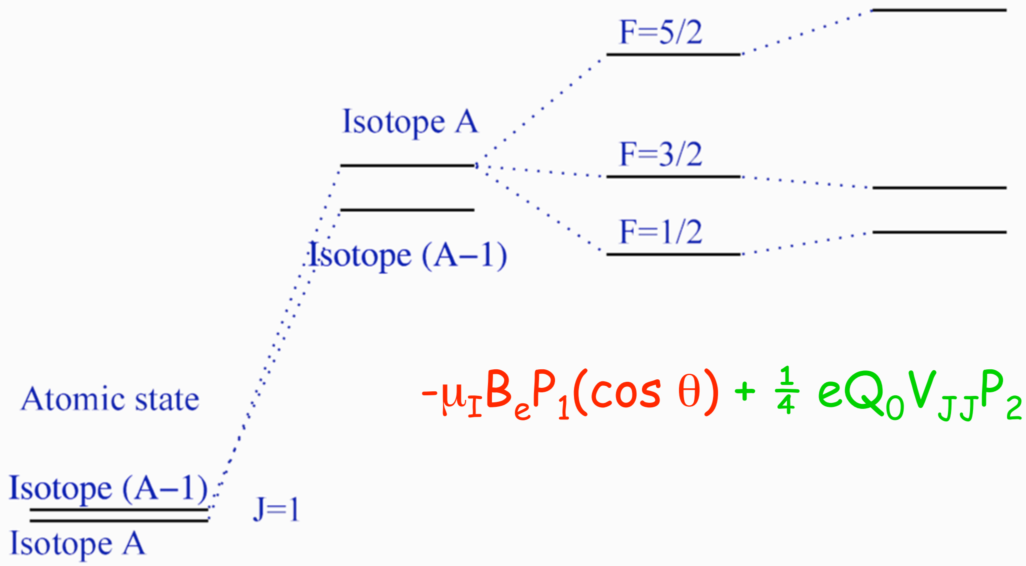

$$-\mu_I B_e P_1(\cos\theta) + \frac{1}{4} eQ_0 V_{JJ} P_2(\cos\theta) + \ldots$$

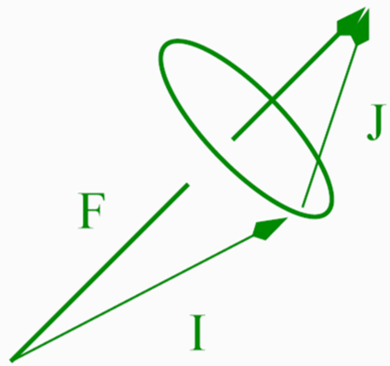

These energy shifts of may be only a few parts per million of the energy of an optical atomic transition.

A single optical transition is split into a number of hyperfine components.

Appearance of hyperfine structure

I = 0 would have single peak

I = 5/2 (Dipole transition: $\Delta F = 0, +/- 1$)

6 peaks spread over 2×10^9 Hz

(transition frequency: 1×10^{15} Hz)

Relative intensities of peaks are determined by the quantum numbers I, J, F.

Relative positions of peaks are determined by I, J_i, J_f, μ_I, Q_s

Not all peaks need be located to determine an unknown I, μ_I, Q_s

Note: centroid position of ^{26}Al is shifted relative to ^{27}Al: the isotope shift….

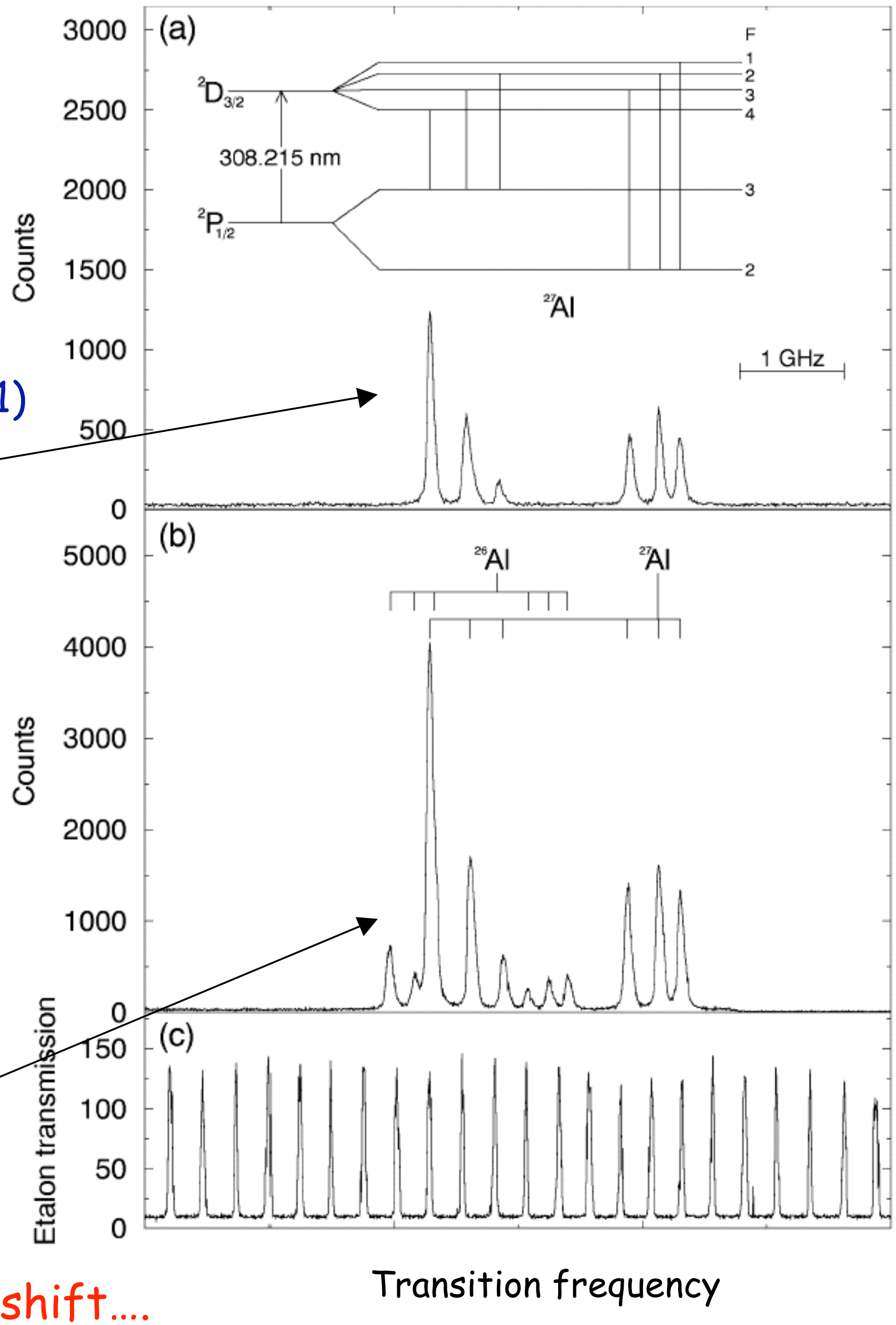

The Isotope Shift

Experimental observation

2 contributions to shift:

$$\delta\nu_i^{A,A'} = \delta\nu_{i,MS}^{A,A'} + \delta\nu_{i,FS}^{A,A'}.$$

Mass Shift due to change in the nucleus recoil kinetic energy (partly related to the change in electron reduced mass).

Field shift due to finite volume of nuclear charge – the nucleus is not a point-like object.

Laser–fluorescence of free atoms

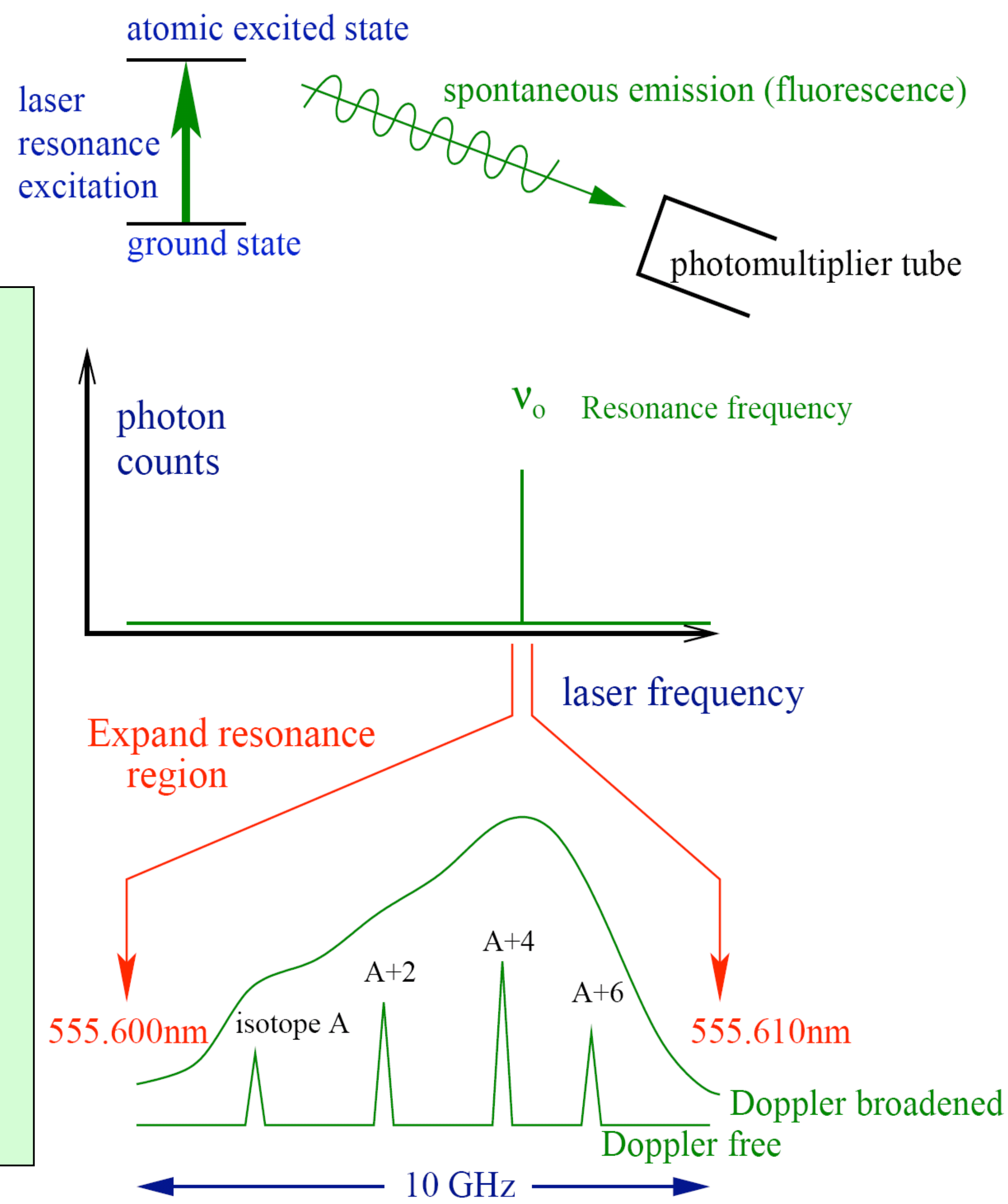

Mass Shift

Kinetic energy (nucleus + electrons) $T = \frac{P_n^2}{2M_n} + \sum_i \frac{p_i^2}{2m_e}$

But in centre of mass frame $\mathbf{P_n} = -\sum_\mathbf{i} \mathbf{p_i}$

Thus nucleus kinetic energy is $T_{nuc} = \frac{1}{2M_n}\sum_i \mathbf{p_i^2} + \frac{1}{2M_n}\sum_{i\neq j}(\mathbf{p_i}\cdot\mathbf{p_j})$

Energy change between two isotopes A, A′ $\delta T_{nuc} = \frac{1}{2m_u}\left(\frac{A'-A}{AA'}\right)\left(\sum_i(\mathbf{p_i})^2 + \sum_{i>j}(2\mathbf{p_i}\cdot\mathbf{p_j})\right)$

"normal" "specific"

$$\delta\nu_{MS}^{A,A'} = (N+S)\left(\frac{A-A'}{AA'}\right).$$

$$N = \frac{m_e}{m_u}\nu_0$$

S must be evaluated by experiment or calculation - difficult

Field Shift

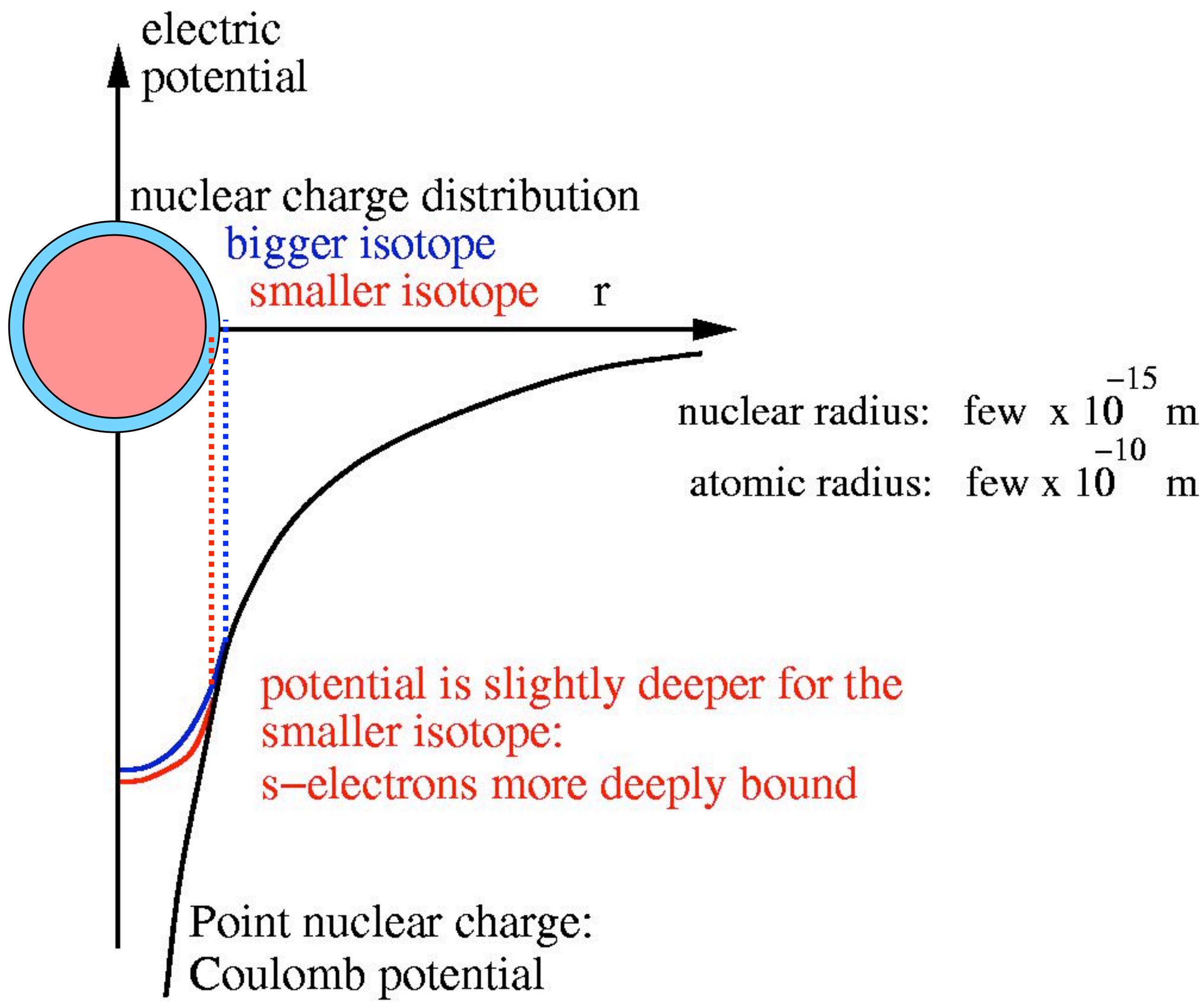

electric
potential
nuclear charge distribution
bigger isotope
smaller isotope
r
nuclear radius: few x 10^{-15} m
atomic radius: few x 10^{-10} m
potential is slightly deeper for the
smaller isotope:
s–electrons more deeply bound
Point nuclear charge:
Coulomb potential

Electrostatic energy of nuclear charge in potential due to electrons

$$E = \int_0^\infty \rho_n(\mathbf{r}) V_e(\mathbf{r}) \mathrm{d}\tau$$

Assuming constant electron density in region of nucleus, Gauss's Law gives

$$V_e(r) = \rho_e r^2 / 6\epsilon_0 \qquad \text{where} \qquad \rho_e = e|\ \psi(0)\ |^2$$

Giving: $$E = \int_0^\infty \rho_n(\mathbf{r}) \rho_e r^2 / 6\epsilon_0 \mathrm{d}\tau$$

Now remember $$\langle r^2 \rangle = \frac{1}{Ze} \int_0^\infty \rho_n(\mathbf{r}) r^2 \mathrm{d}\tau$$

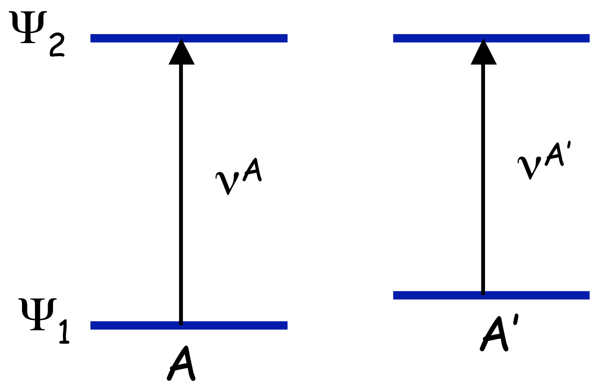

Transition energy difference between isotopes A and A′

$$\delta E = \frac{Ze^2}{6\epsilon_0} \Delta\ |\ \psi(0)\ |^2\ \delta \langle r^2 \rangle^{A,A'}$$

Field Shift component of Isotope Shift = $F\ \delta \langle r^2 \rangle^{A,A'}$

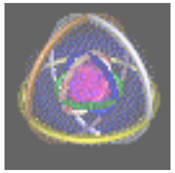

Summary of Isotope Shift and Hyperfine Structure

Isotope shift of atomic transition

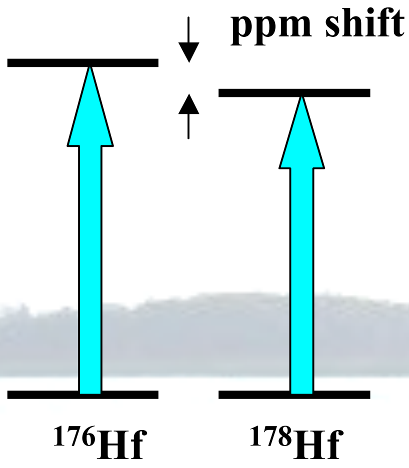

Analysis yields the change in nuclear mean square charge radius

↓

Nuclear size, static and dynamic deformations

Hyperfine structure of atomic transition

(Isotope shift found using centroids of hyperfine multiplet)

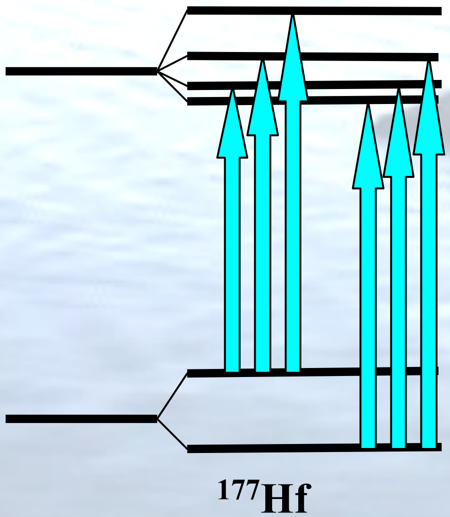

Nuclear spin I

Magnetic moment μ

Quadrupole moment Q_s

Factors controlling $\delta \langle r^2 \rangle$

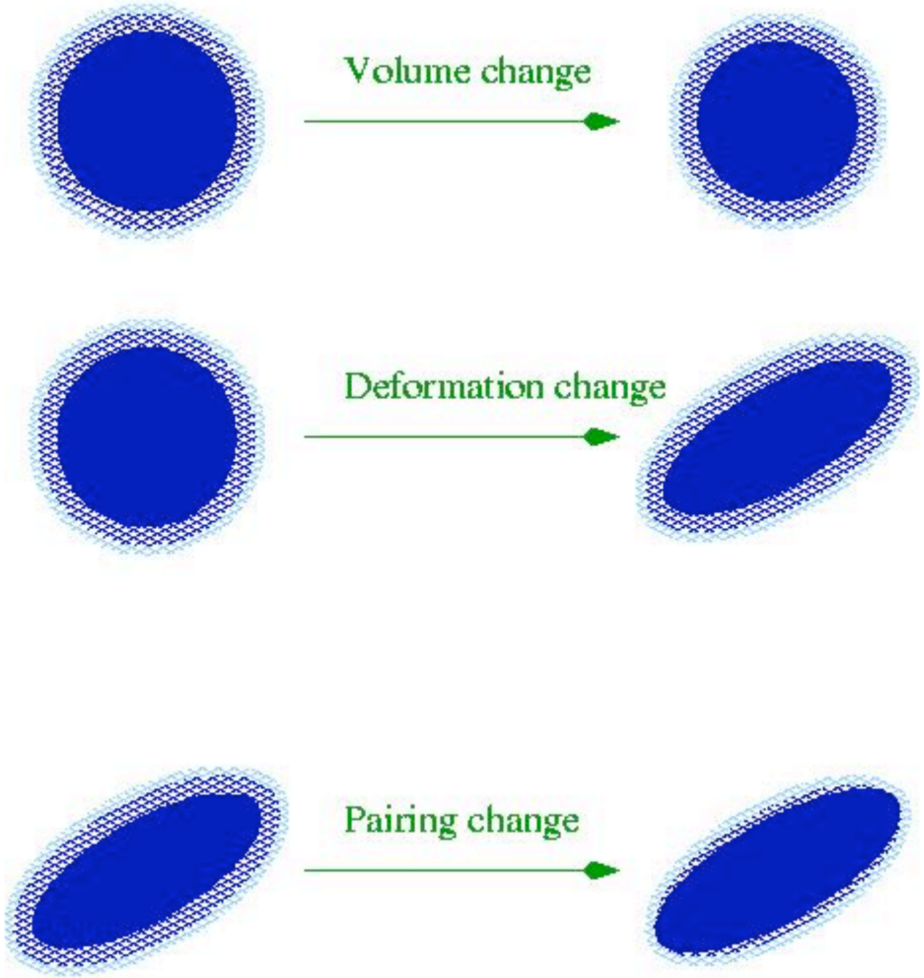

(change in surface diffuseness)

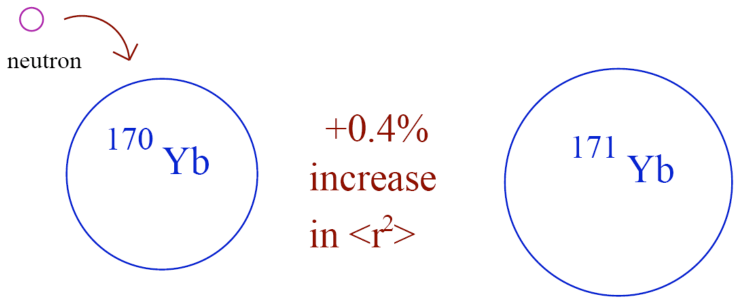

(small, but easily detectable by laser spectroscopy)

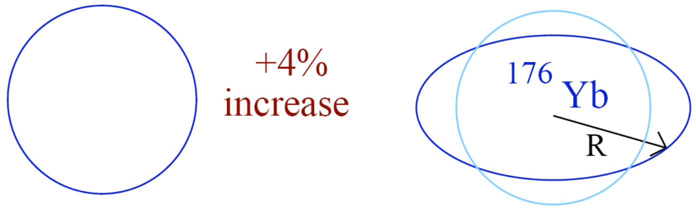

$$\langle r^2 \rangle = \langle r^2 \rangle_0 \left(1 + 5/4\,\pi \left[\langle \beta_2^2 \rangle + \langle \beta_3^2 \rangle + \ldots \right\} \right)$$

The contributions here may be

STATIC – determined by nuclear shape

or DYNAMIC – determined by fluctuations of the nuclear surface

Mean square charge radii

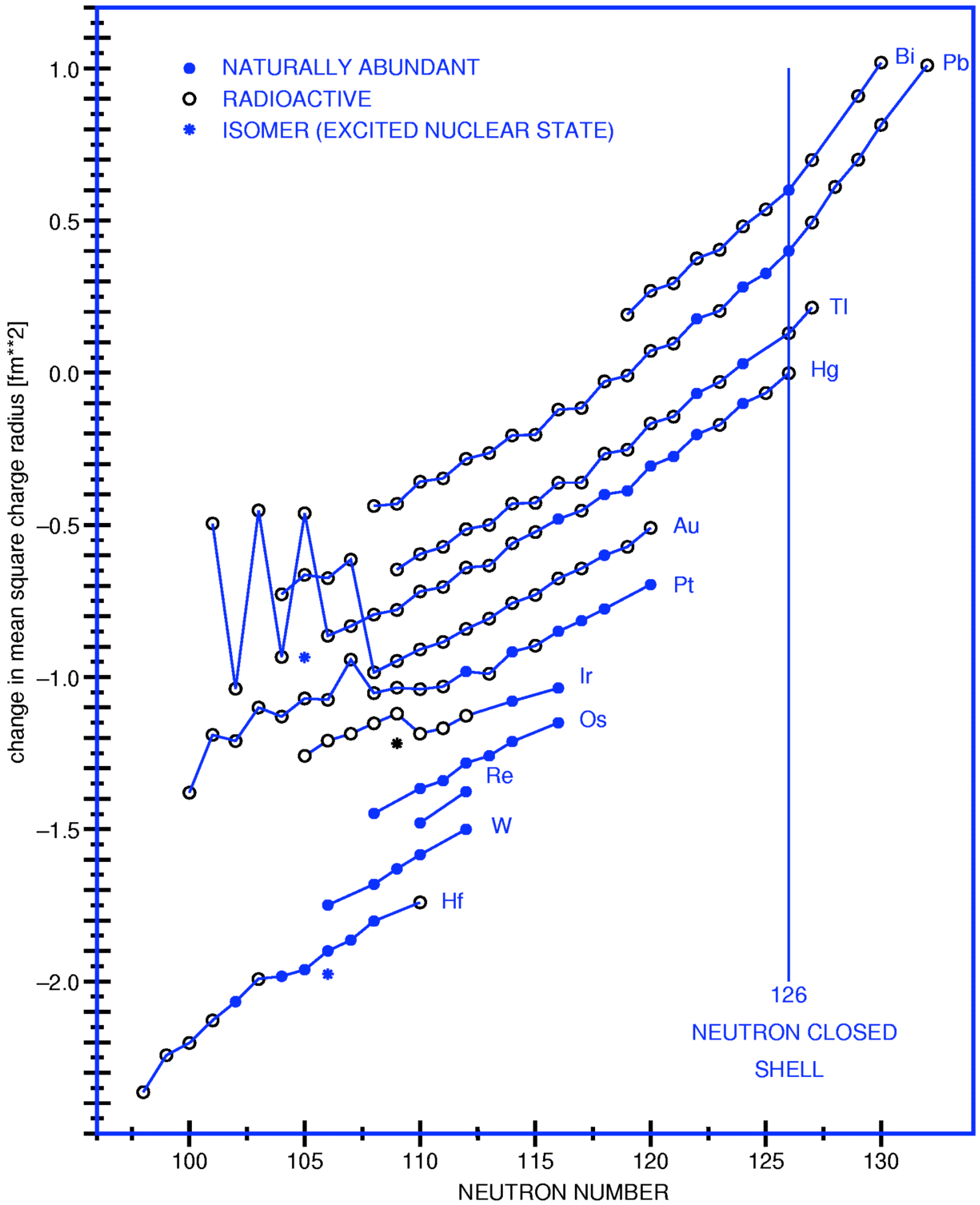

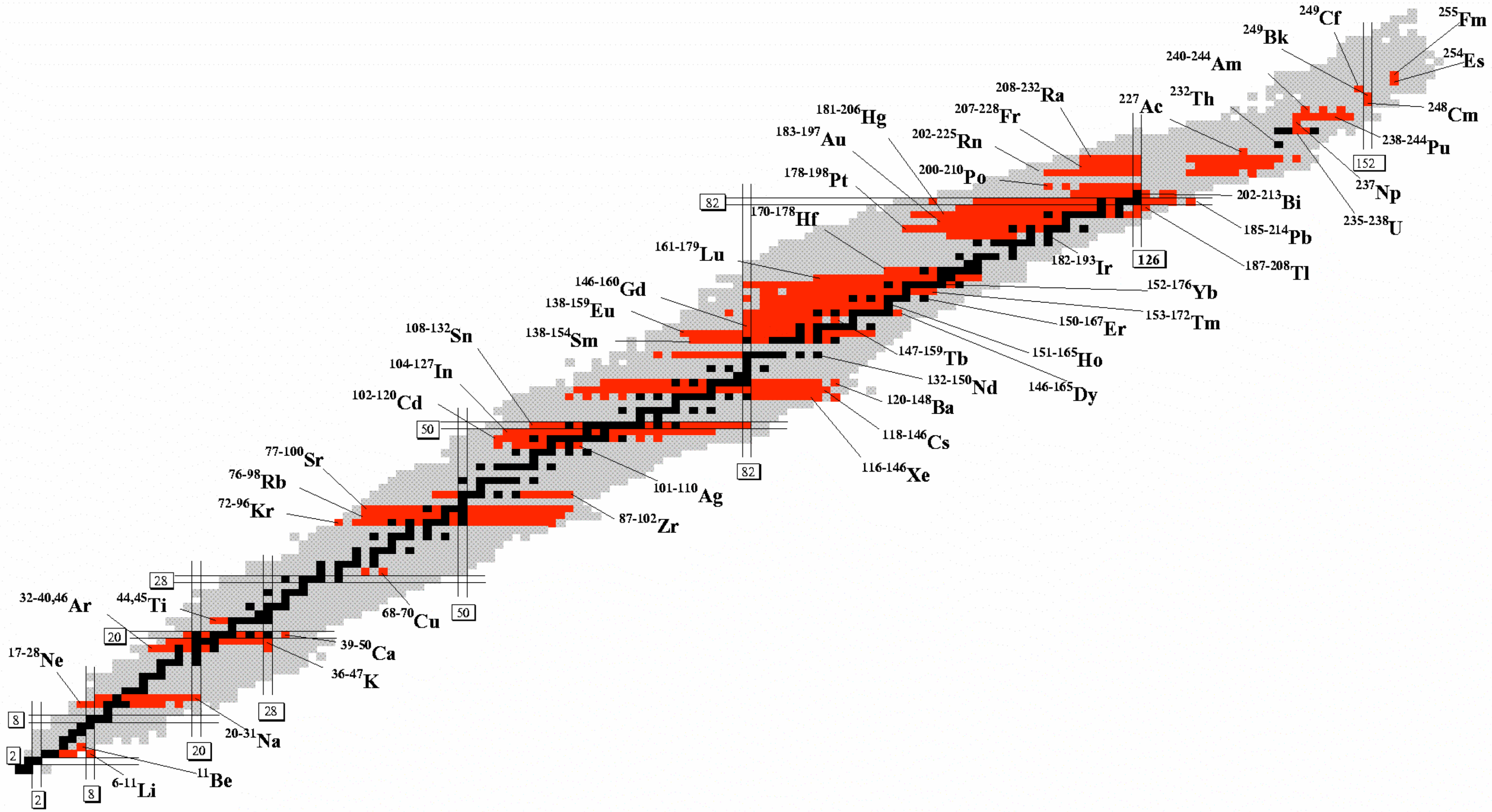

249Cf
255Fm
249Bk
254Es
240-244Am
208-232Ra
232Th
227Ac
248Cm
207-228Fr
181-206Hg
238-244Pu
183-197Au
202-225Rn
152
200-210Po
178-198Pt
237Np
202-213Bi
82
170-178Hf
185-214Pb
235-238U
182-193Ir
126
187-208Tl
161-179Lu
146-160Gd
152-176Yb
138-159Eu
153-172Tm
150-167Er
138-154Sm
108-132Sn
151-165Ho
147-159Tb
104-127In
132-150Nd
146-165Dy
102-120Cd
120-148Ba
50
118-146Cs
82
77-100Sr
116-146Xe
101-110Ag
76-98Rb
72-96Kr
87-102Zr
28
68-70Cu
50
32-40,46Ar
44,45Ti
20
39-50Ca
36-47K
17-28Ne
28
8
20-31Na
20
2
11Be
6-11Li
2
8

1.3 Lasers and laser spectroscopy

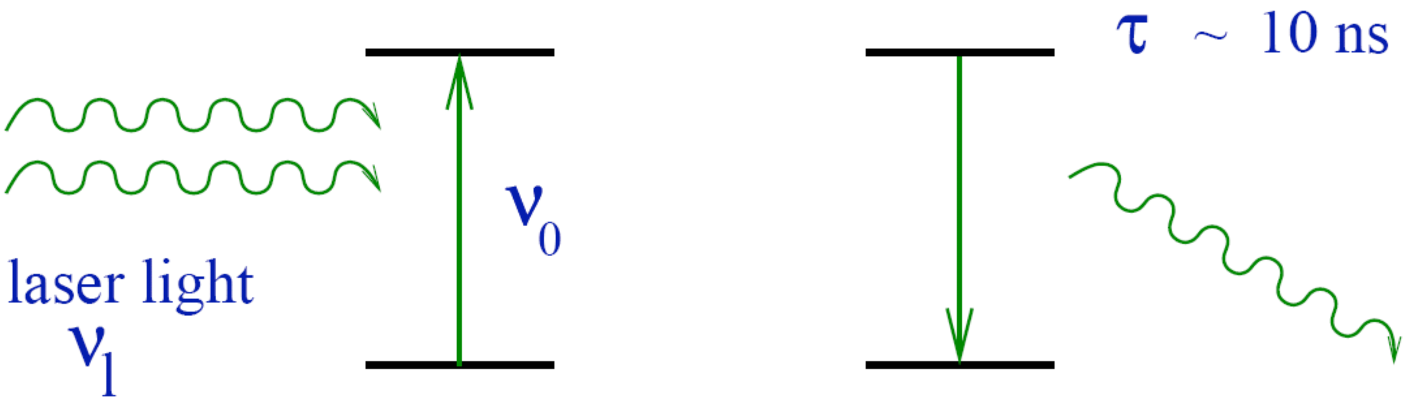

Resonant absorption ($\nu_l = \nu_0$) Spontaneous emission

$$\sigma = \frac{3\lambda^2}{2\pi}$$ (much larger than size of atom)

Natural linewidth $\Delta\nu = 1/2\pi\tau$ (Heisenberg uncert.)

~ 16 MHz

single–mode CW laser bandwidth < 1MHz

Dye lasers:

* Wavelengths from 400nm to IR
* Can be frequency-doubled (200nm – 400nm)
* Bandwidth < 1 MHz
* Sufficient power to "saturate" a transition

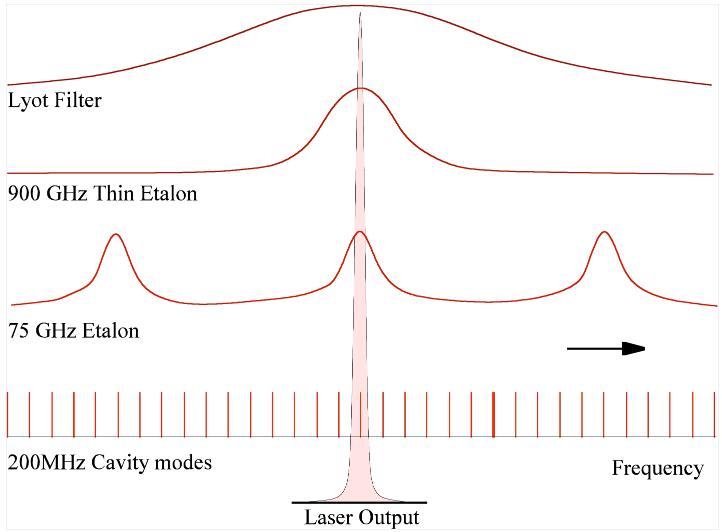

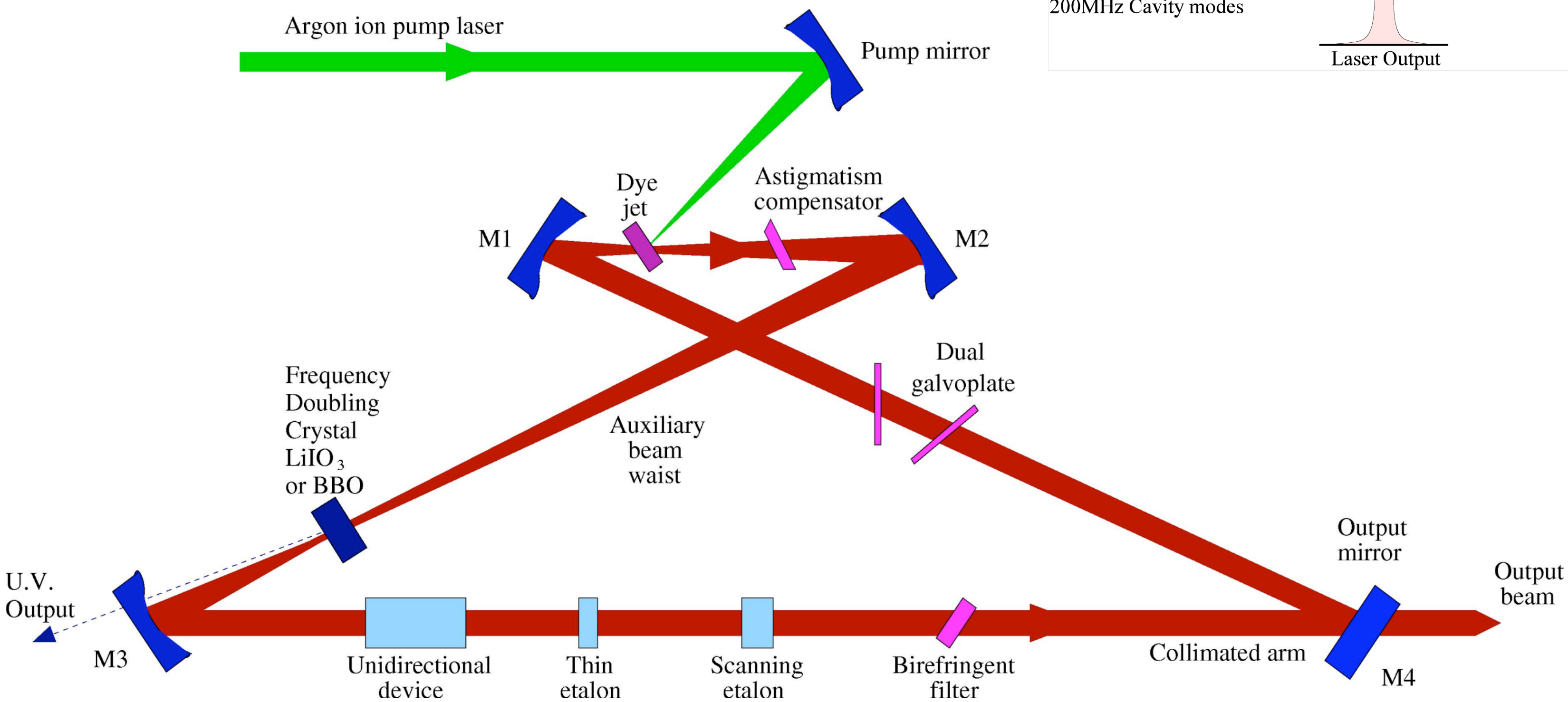

Main problem in laser spectroscopy:

Doppler broadening (inhomogeneous) — atomic vapour: Maxwell–Boltzmann velocity distribution

Resonance of atom shifted to $\nu_0 (1 + v_x / c)$

Velocity distribution (Gaussian) :

$$P (v_x) = \exp (-m v_x^2 / 2 k T)$$

$$\mathrm{FWHM} = \sqrt{8kT \ln 2 / mc^2} \sim 1 \text{ GHz}$$

Doppler–free techniques required.

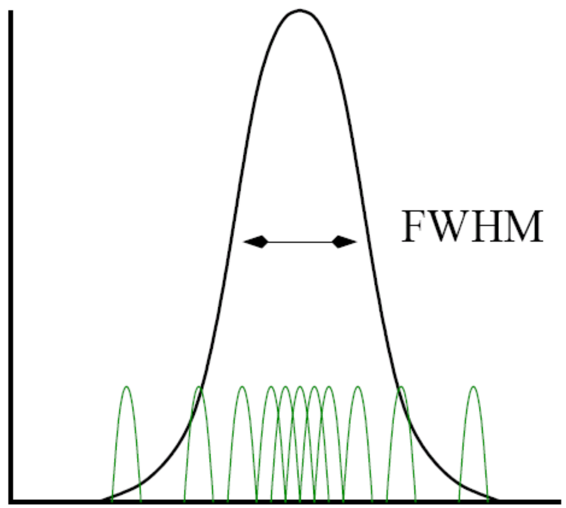

* Collinear-beams method is Doppler broadening-free and has sufficient sensitivity to allow measurements on radioactive isotopes.

1.4 Collinear-beams laser spectroscopy

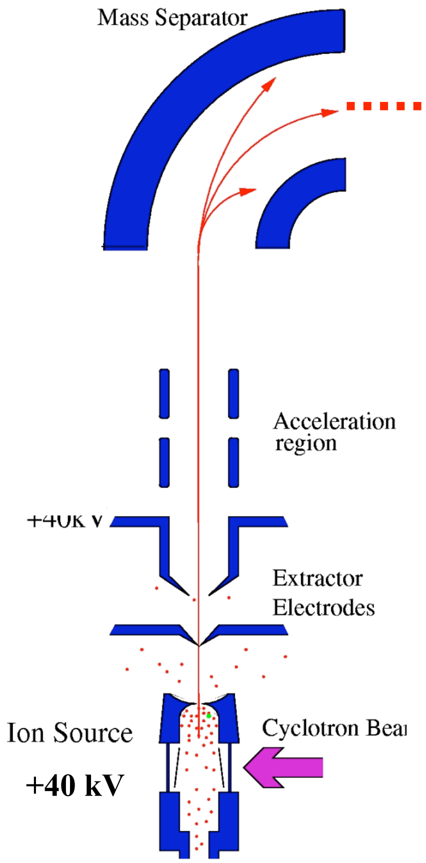

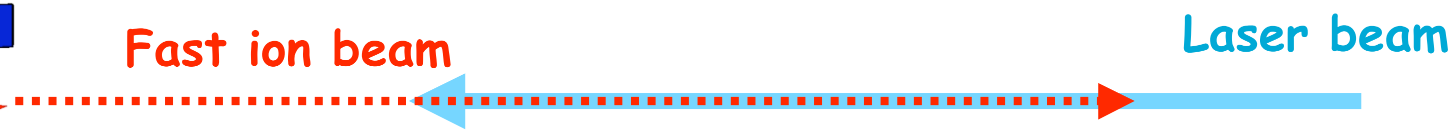

Principle behind the collinear beams method

Adding a fixed energy to each ion in the sample

→ increases the velocity
but
reduces the velocity spread

An example:
Dropping a particle through a fixed distance

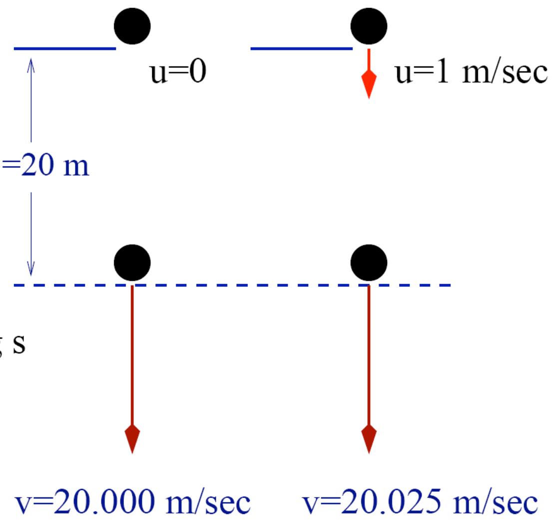

$v^2 = u^2 + 2\,g\,s$

High sensitivity: all ions in the beam contribute to the fluorescence signal when the laser frequency is on resonance with the optical transition

Count rates for low-flux ion beams

Signal (laser on resonance) =
1 photon detected per 1,000 ions in beam

Background (laser light scatter) = 200 photons / second

Low-flux beams (1,000 ions / sec): background must be suppressed to see signal.

Details of the laser-ion interaction region

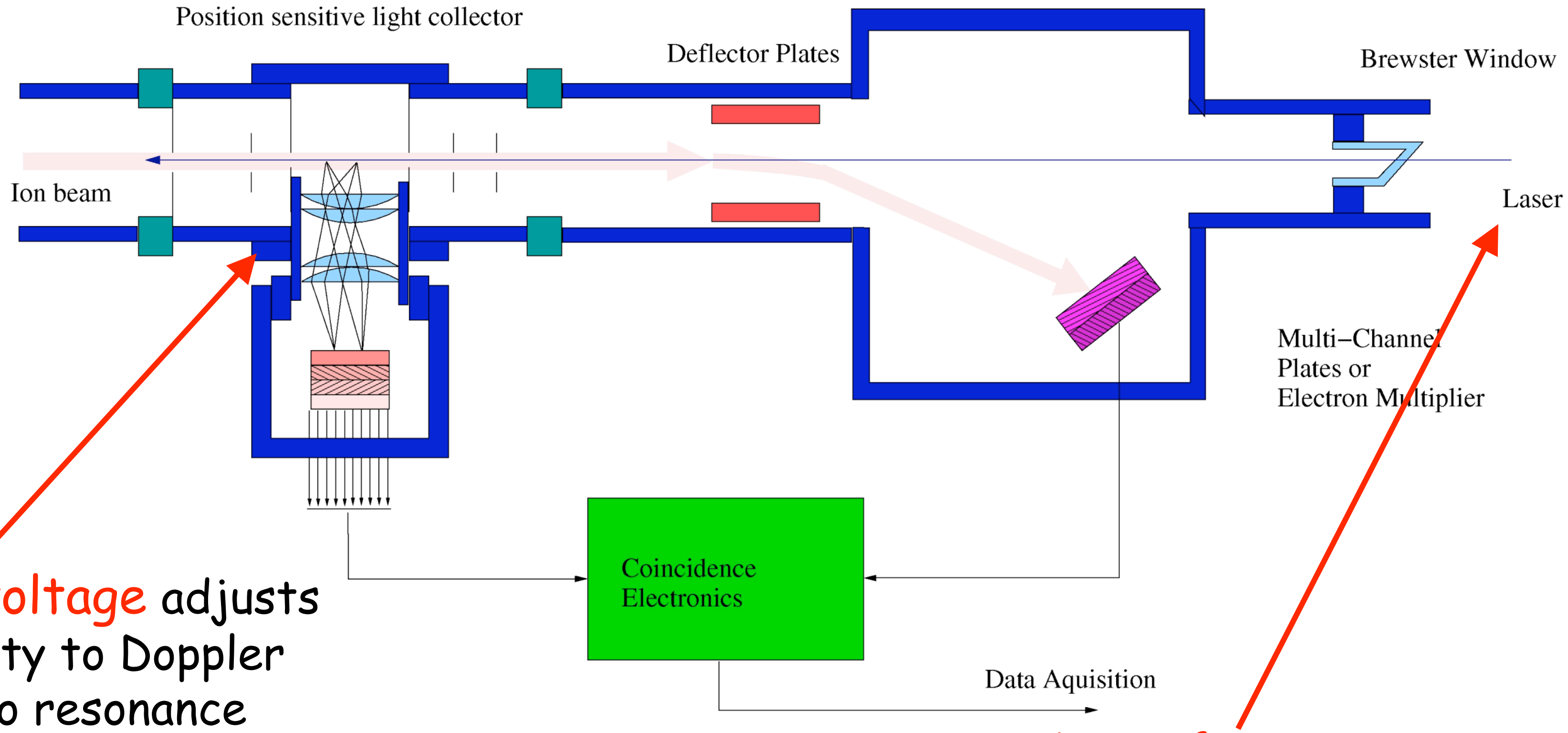

Tuning voltage adjusts ion velocity to Doppler shift it to resonance with locked laser

Laser frequency "locked" to a reference for long-term stability

(Arrangement shown above is for the photon-ion coincidence detection method)

Isomer shift in an optical transition

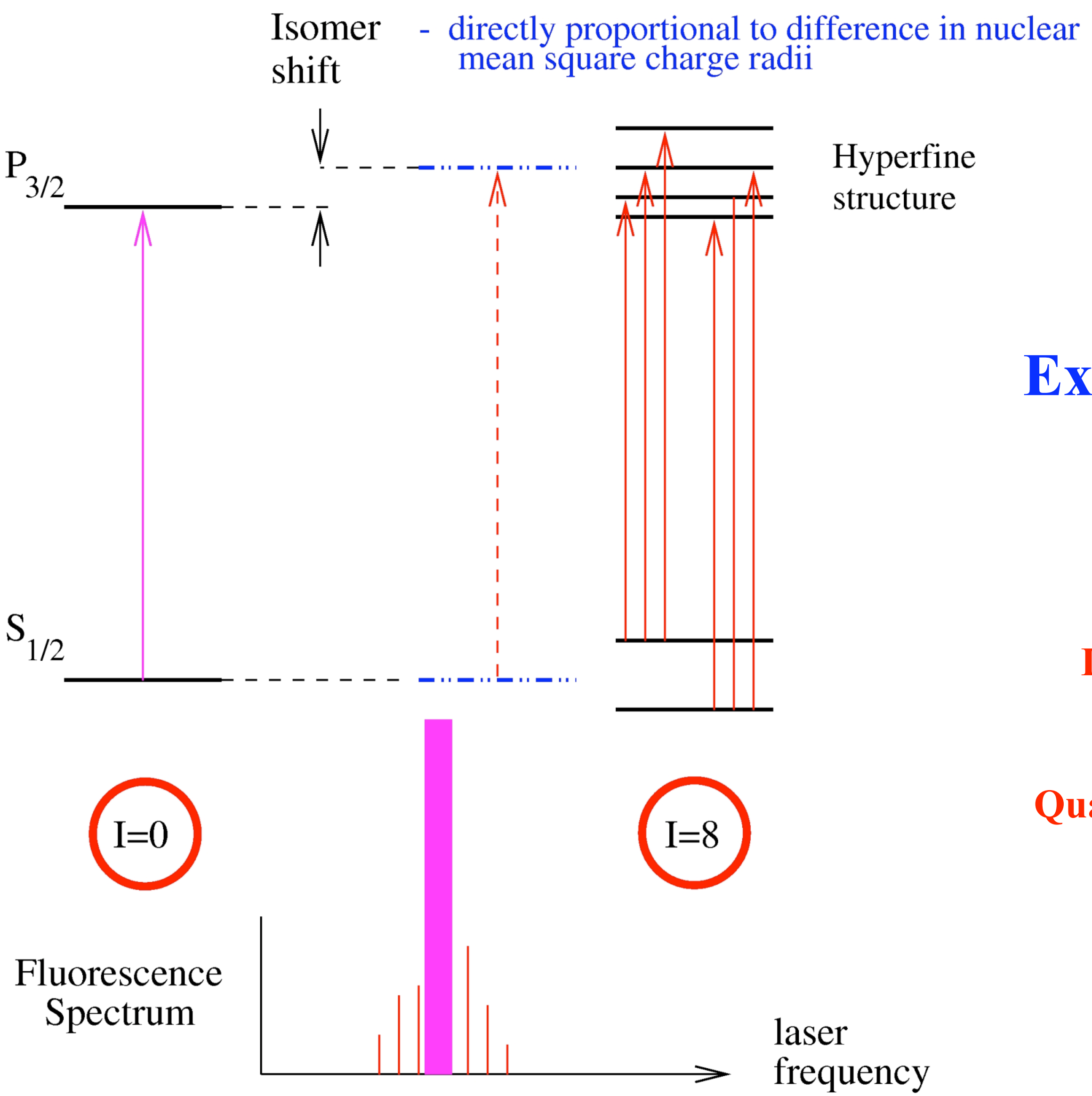

Experimental problems:

Small Hyperfine structure

Small isomer shift

Large fraction of beam is in the nuclear ground state

Quadrupole interaction can change order of components

Ionic Ytterbium Spectra (329.938nm)

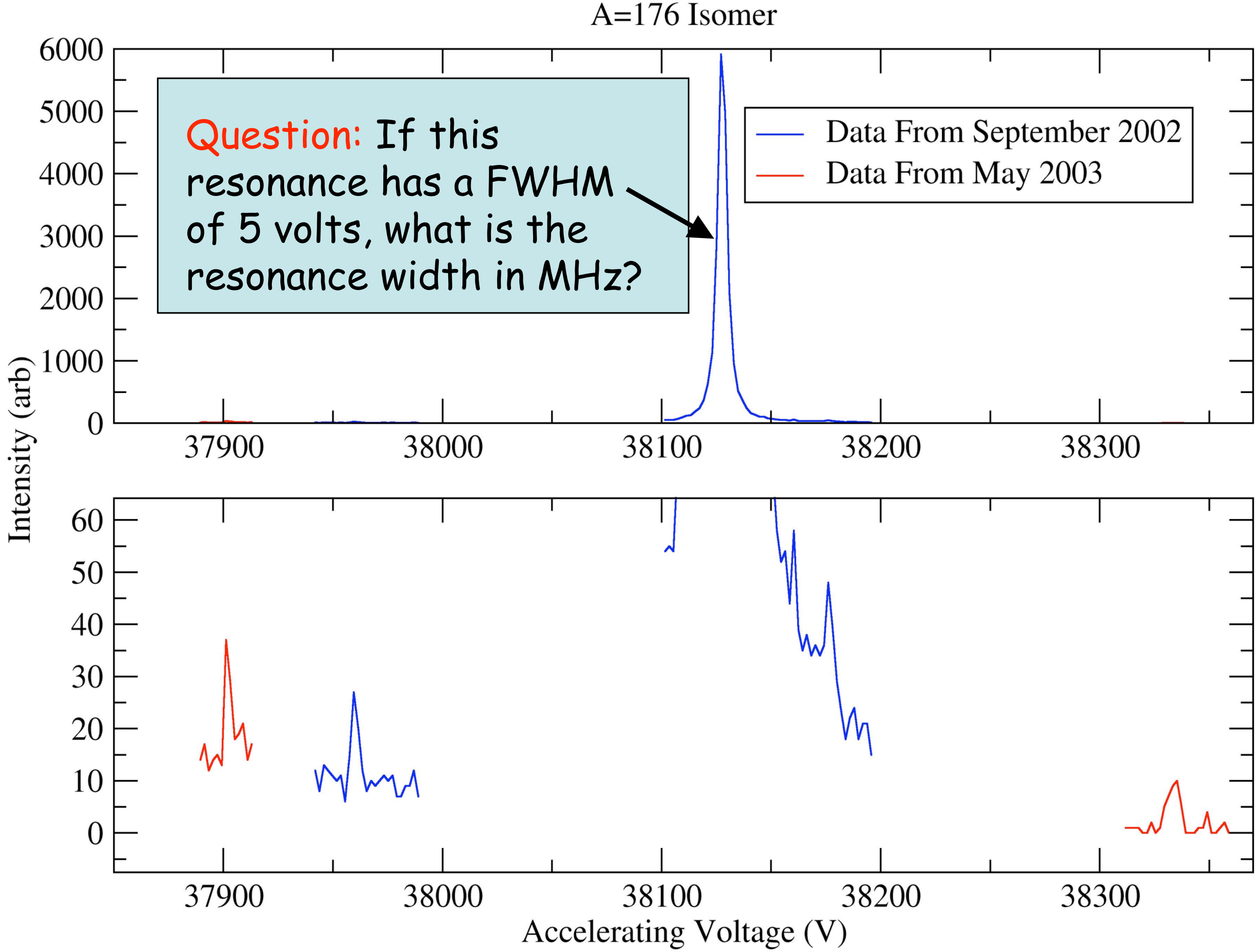


End of Lecture 1

Simplified schematic of MBD-200

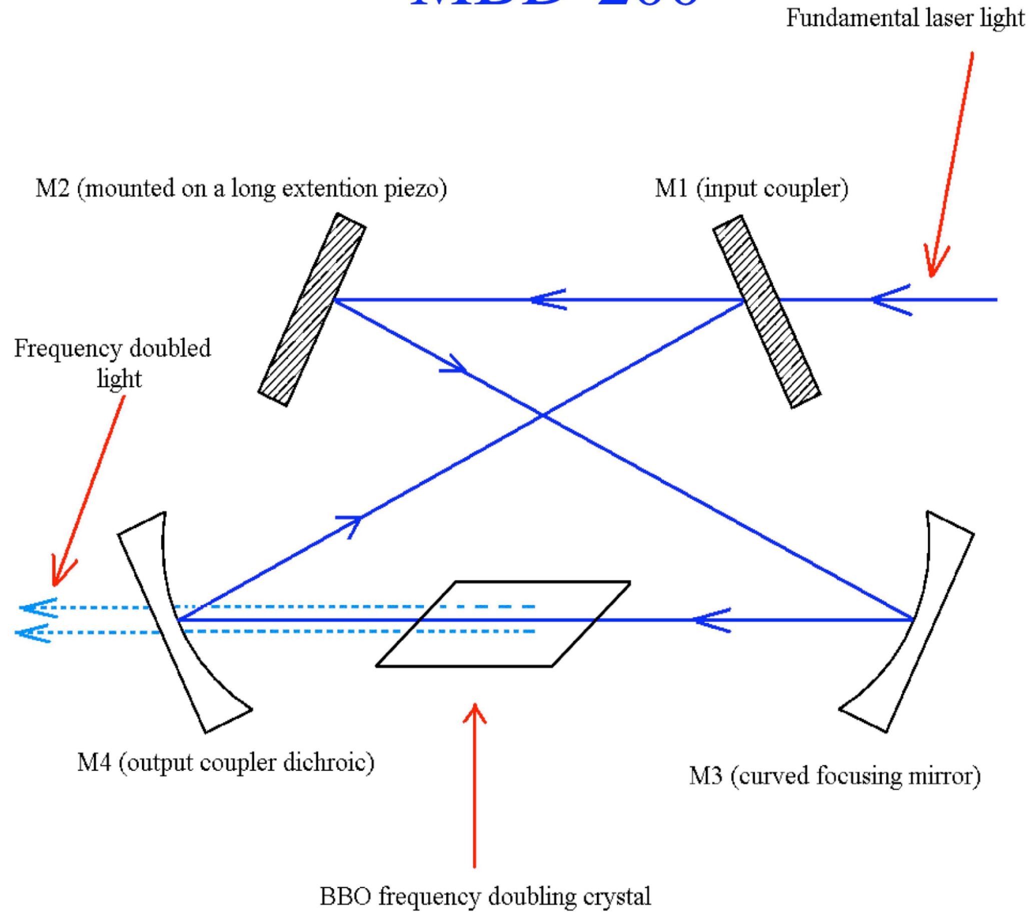


MELLES GRIOT